NeuroImage: Clinical 21 (2019) 101609

Contents lists available at ScienceDirect

NeuroImage: Clinical

journal homepage: www.elsevier.com/locate/ynicl

Hippocampal vascularization patterns: A high-resolution 7 Tesla time-of-flight magnetic resonance angiography study

Spallazzi Marco[a,*], Dobisch Laura[b,c], Becke Andreas[b,c], Berron David[b,c], Stucht Daniel[d], Oeltze-Jafra Steffen[e], Caffarra Paolo[a], Speck Oliver[c,d,f,g], Düzel Emrah[b,c,h,**]

[a] Department of Neuroscience, University of Parma, Italy
[b] Institute for Cognitive Neurology and Dementia Research, University of Magdeburg, Germany
[c] German Center for Neurodegenerative Diseases, Magdeburg, Germany
[d] Department of Biomedical Magnetic Resonance, Otto-von-Guericke University Magdeburg, Germany
[e] Department of Simulation and Graphics, University of Magdeburg, Germany
[f] Leibniz Institute for Neurobiology, Magdeburg, Germany
[g] Center for Behavioral Brain Sciences, Magdeburg, Germany
[h] Institute of Cognitive Neuroscience, Univ. College London, London, United Kingdom

ARTICLE INFO

Keywords:
7 T MRI
Hippocampal vascularization
Hippocampus
MR angiography
Neuroanatomy

ABSTRACT

Considerable evidence suggests a close relationship between vascular and degenerative pathology in the human hippocampus. Due to the intrinsic fragility of its vascular network, the hippocampus appears less able to cope with hypoperfusion and anoxia than other cortical areas. Although hippocampal blood supply is generally provided by the collateral branches of the posterior cerebral artery (PCA) and the anterior choroidal artery (AChA), different vascularization patterns have been detected postmortem. To date, a methodology that enables the classification of individual hippocampal vascularization patterns *in vivo* has not been established. In this study, using high-resolution 7 Tesla time-of-flight angiography data (0.3 mm isotropic resolution) in young adults, we classified individual variability in hippocampal vascularization patterns involved in medial temporal lobe blood supply *in vivo*. A strong concordance between our classification and previous autopsy findings was found, along with interesting anatomical observations, such as the variable contribution of the AChA to hippocampal supply, the relationships between hippocampal and PCA patterns, and the different distribution patterns of the right and left hemispheres. The approach presented here for determining hippocampal vascularization patterns *in vivo* may provide new insights into not only the vulnerability of the hippocampus to vascular and neurodegenerative diseases but also hippocampal vascular plasticity after exercise training.

1. Introduction

Since the studies of Spielmeyer (1925) and Uchimura (1928), hippocampal vascularization has been considered one of the possible main determinants involved in hippocampal degeneration. Although Spielmeyer's vascular theory on Ammon's horn sclerosis (Spielmeyer, 1927) was refuted in subsequent years (Blümcke et al., 1999; Rothman, 1984; Vogt and Vogt, 1937), some observations that emerged from his work are still debated (Duvernoy, 2005). The intrahippocampal vascular network has apparent "vascular vulnerability" with a relatively small number of capillary anastomoses and an inadequate ability to cope with hypoperfusion (Scharrer, 1940). Compared with the isocortex, the hippocampal allocortex displays significant differences not only in layer number and composition but also in vascularization (Muller and Shaw, 1965; Ravens, 1974; Duvernoy et al., 1981). The long tangential course of arteries and veins in the hippocampus differs from that of the isocortical vessels, which are usually short and perpendicular to the surface with a palisade aspect. The penetration of large intrahippocampal arteries at a perpendicular angle combined with a long course and few anastomoses may, at least partially, explain the particular vulnerability of hippocampal tissue to anoxia (Klosovskii, 1963; Marinkovic et al., 1992).

Arterial vascularization of the hippocampus is dependent on the collateral branches of the posterior cerebral artery (PCA) and to a lesser degree, the anterior choroidal artery (AChA) (Erdem et al., 1993). Numerous variations concerning the origin of hippocampal arteries and

* Correspondence to: M. Spallazzi, Department of Neuroscience, University of Parma, Via Gramsci n. 14, 43126 Parma, Italy.
** Correspondence to: E. Düzel, German Center for Neurodegenerative Diseases, Magdeburg Site, Leipziger Str 44, 39120 Magdeburg, Germany.
E-mail addresses: mspallazzi@ao.pr.it (M. Spallazzi), emrah.duezel@dzne.de (E. Düzel).

https://doi.org/10.1016/j.nicl.2018.11.019
Received 22 May 2018; Received in revised form 3 August 2018; Accepted 18 November 2018
Available online 19 November 2018

the single or mixed contributions of the two main vessels to hippocampal blood supply have been described. In fact, if hippocampal arteries mainly arise from the PCA, the contribution of the AChA is highly variable and not always present (Marinkovic et al., 1999; Morandi et al., 1996; Gastaut and Lammers, 1961). The number of hippocampal arteries is also variable with the particular possibility of multiple posterior hippocampal arteries.

Current knowledge of hippocampal vascularization is based on very old histological studies and more recent neurosurgical autopsy studies. In these later studies, the renewed interest in epilepsy surgery and methodological and technological upgrades in neurosurgery have led to renewed attention to the hippocampal region, a frequent target of surgery for intractable temporal lobe epilepsy. Microneurosurgery cannot be performed without an accurate knowledge of the complex macro- and microanatomy of the area, a basic requirement for approaching medial temporal structures in a way that preserves surrounding neural tissues (Wen et al., 1999).

Hippocampal arteries are named according to their territories: the anterior hippocampal artery (AH) supplies the hippocampal head and the uncus, whereas the middle and posterior hippocampal arteries (MH and PH, respectively) vascularize the hippocampal body and tail, respectively. High interindividual variability in the number and distribution of hippocampal arteries resist systematization based only on these aspects, and systematization has hence been considered impracticable and unnecessary in previous postmortem studies (Erdem et al., 1993; Marinkovic et al., 1992). However, the origins of hippocampal arteries differ in terms of the parental vessels that arise from distinct PCA or AChA branches. In the literature, some attempts to classify hippocampal vascularization based on the different origins of the hippocampal arteries have been performed and have identified more stable and reproducible patterns of vascularization. According to these observations, Erdem and colleagues (Erdem et al., 1993) analyzed 30 hemispheres and divided the origins of hippocampal arteries into the five following groups: Group A - mixed origins of hippocampal arteries (AChA + PCA), which is the most frequent type (57%); Group B - mainly from the branches of the PCA, in particular from all the inferior temporal arteries (27%); Group C - mainly from branches of the PCA, in particular from the anterior inferior temporal artery (10%); Group D - mainly from the PCA, directly from the PCA or a common trunk (CT) from the PCA (3%); and Group E - mainly from the AChA (3%). More recent studies have been consistent with Erdem and colleagues' results, confirming the high variability in hippocampal blood supply (Fernandez-Miranda et al., 2010; Huther et al., 1998). Even considering only the role of the PCA in the vascularization of the medial temporal lobe, different temporal cortical branches and patterns have been described. Haegelen et al. (2012), starting from Zeal and Rhoton (1978), carried out a microanatomical study of the temporal branches of the PCA and proposed a revised classification of their findings. Based on their analysis of 40 hemispheres, they classified the arteries of the inferior temporal branches of the PCA into the following three patterns: the first pattern always includes the anterior temporal artery (AT) and the posterior temporal artery (PT), without the anterior hippocampal artery (AH); the second pattern always comprises the AH, AT and PT; and the third pattern always includes a common trunk (CT) from which all inferior temporal cortical branches arise. The first pattern is the most frequent (57.5%), followed by the second (22.5%) and third patterns (20%).

Until now, unlike the large production of structural and functional studies of the human hippocampus, no neuroimaging studies have investigated hippocampal vascular anatomy in detail. The main reason underlying this neglect may be the small size of hippocampal vessels, with the diameter of hippocampal arteries ranging from 0.2 to 0.8 mm (mean 0.5 mm). Today, 7 Tesla (7 T) time-of-flight magnetic resonance (TOF MR) angiography allows imaging of these small vessels and provides a time-efficient method to achieve high-resolution angiograms without venous contamination (Heverhagen et al., 2008; Zang et al., 2015).

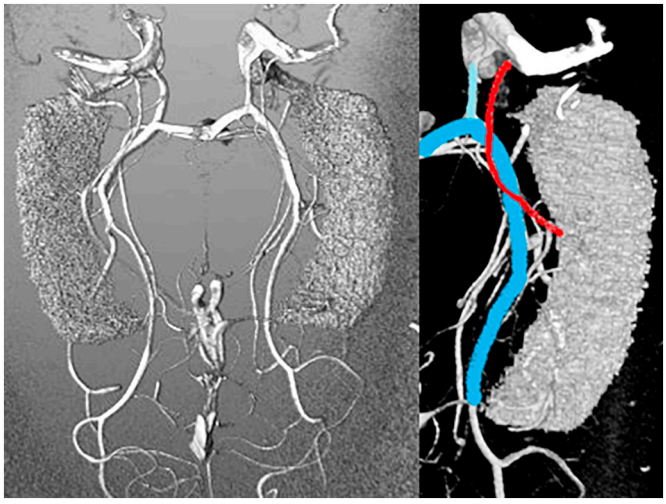

Fig. 1. On the left: a TOF MRA reconstruction with the hippocampal mask; on the right: main vessels involved in the hippocampal supply; posterior cerebral artery (light blue), anterior choroidal artery (red), posterior communicating artery (cyan).

In this study, using high-resolution 7 T TOF MR angiography data (0.3 mm isotropic resolution), we aimed to detect hippocampal vascularization patterns *in vivo* to compare and validate our results with previously published autopsy observations (Figs. 1 and 2). The ability to assess individual differences in hippocampal vascularization *in vivo* could provide (in the near future) a new opportunity to understand individual differences in hippocampal degeneration and plasticity.

2. Materials and methods

2.1. Study population

The study was conducted at the German Center for Neurodegenerative Diseases in Magdeburg, the Institute of Cognitive Neurology and Dementia Research of the Otto-von-Guericke University Magdeburg and the Leibniz Institute for Neurobiology in Magdeburg, Germany. In this study, we analyzed 7 T TOF MR angiography (MRA) data from 41 healthy young adult humans (25 females, 19–34 years) who underwent a 7 T MRI for research purposes.

Inclusion criteria comprised the absence of known neurological or psychiatric conditions. All participants signed written consent forms and received monetary compensation for their participation. The protocol was approved by the Ethics Committee of the Otto-von-Guericke University Magdeburg, Germany.

2.2. MR imaging protocol

The MR acquisition was performed on a 7 T whole body system (Siemens, Erlangen, Germany) using a 32-channel receiving head coil (Nova Medical, Wilmington MA, USA). The protocol included T1-weighted MPRAGE acquisition (whole brain, 0.6 mm isotropic resolution, 288 slices, TR: 2500 ms, TA: 14:02). The other sequence acquired, 7 T TOF angiography, was the most important for this study. This sequence exploits the highly unsaturated longitudinal magnetization of flowing blood that enters the measurement volume, leading to much higher signal intensity than saturated stationary brain tissue. Thus, positive vessel contrast is achieved. Selectivity to arterial vessels is achieved through distal saturation. TOF was scanned with 0.3 mm isotropic resolution, 4 slabs of 40 slices, TR: 24 ms, and TA: 17:10. The TOF measurement volume covered the hippocampal area, which allowed us to achieve very high spatial resolution while keeping the

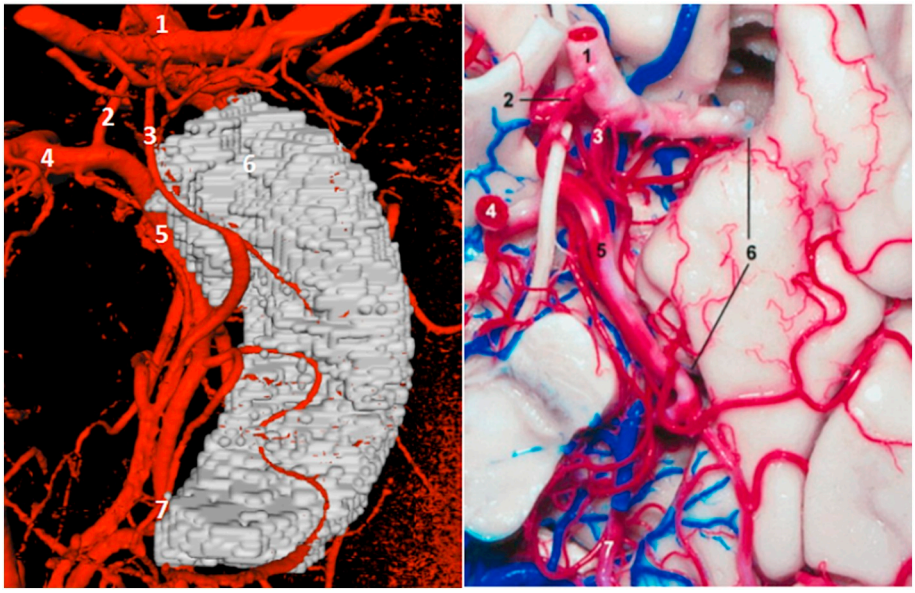

Fig. 2. 7 T TOF MRA *vs post mortem* findings. On the left: Mevislab visualization of TOF MRA data. On the right: a *post mortem* analysis of the medial temporal supply (Wen et al., 1999). 1, internal carotid artery; 2, posterior communicating artery; 3, anterior choroidal artery; 4, P1 segment of the posterior cerebral artery; 5, P2 segment of the posterior cerebral artery; 6, uncus; and 7, P3 segment of the posterior cerebral artery.

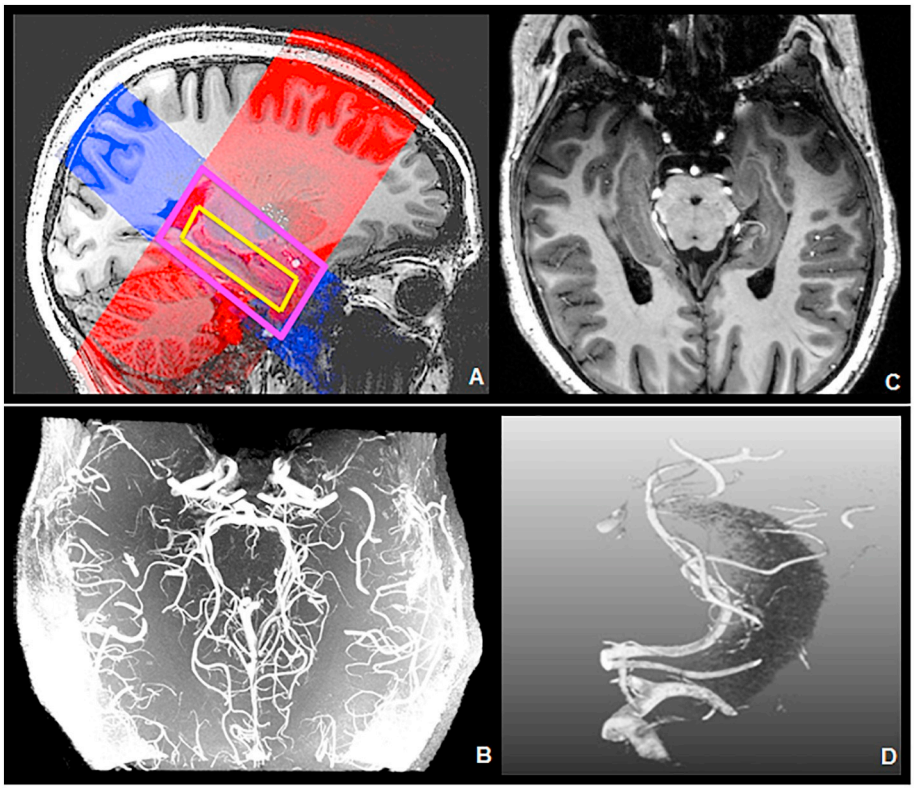

Fig. 3. A) 7 T T1 sequence (grayscale background), 7 T T2 sequence (red), 7 T TOF sequence (blue), hippocampus (yellow). B) 7 T TOF MRA. C) 7 T TOF on 7 T MPRAGE. D) Mevislab reconstruction of 7 T TOF MRA (with the hippocampal mask).

acquisition time as short as possible (Fig. 3).

2.3. Processing & image analysis

Structural masks of the whole hippocampus (left/right) were generated using automated segmentation of the whole brain T1 image using FSL FIRST (Centre for Functional Magnetic Resonance Imaging of the Brain, University of Oxford, see Patenaude et al., 2011). In addition, structural hippocampus masks were manually checked and corrected if necessary using FSLVIEW. Corrected T1 hippocampus masks were coregistered to TOF images using ANTs coregistration algorithms (Avants et al., 2011). For the analysis of the relationship between arteries and brain structures, TOF MRA data were superimposed on the T1 images and viewed in coronal, sagittal and transverse orientations. The classification of hippocampal and PCA patterns using the TOF images was accomplished using MeVisLab (MeVis, Bremen, Germany). The vessels of interest were first reconstructed together with the hippocampal mask to facilitate correct recognition of hippocampal arteries and their relationships with hippocampal structures. Afterwards, vessels were analyzed without hippocampal masks to identify more complex vascular details, such as the anastomosis between AChA and PCA branches. These vascular structures could be further extracted into

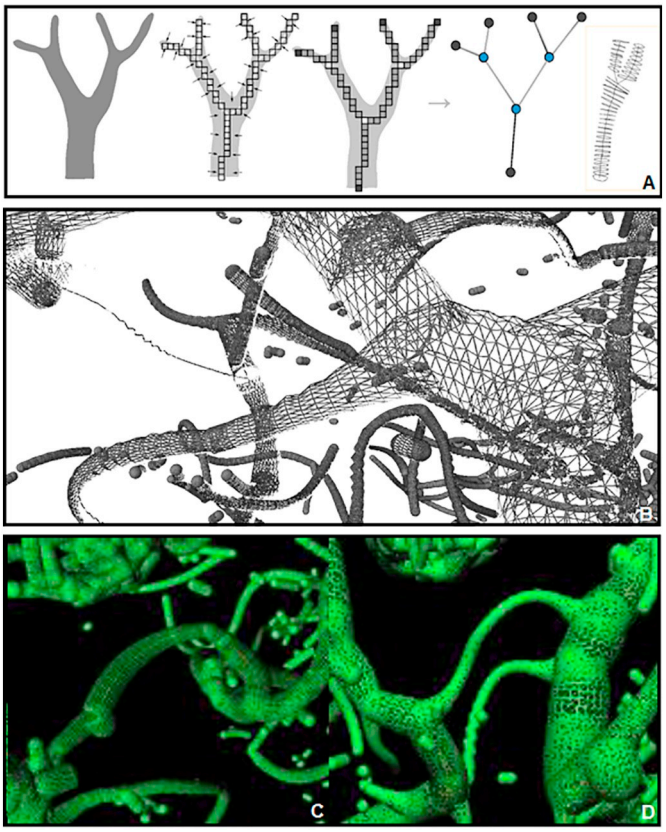

Fig. 4. Vessel skeletonization. A) Procedure to generate skeletons (Selle et al., 2002). B–D) Skeletonization of the PCA branches.

skeletons to gather information about vessel diameters and the branching of the vascular tree, facilitating the PCA branching detection (Fig. 4).

Using direct volume rendering, vessels were clearly visible. An overview of the basic visualization during the analysis task is provided in Fig. 3 D, where the hippocampus was visualized in addition to the vessels of interest; the PCA was the most prominent with its branches penetrating the hippocampus. The fastest visualization technique for vessel analysis involves using a maximum intensity projection (MIP). Here, the brightest voxels in the direction perpendicular to the current plane are displayed. However, this method has limitations, such as the lack of depth information and possible occlusions. Due to different signal intensities, the contrast was individually adjusted for each subject. The signal-to-noise ratio poses a challenge for the adaptation of contrast. Moreover, MIP visualizations provide an easier and better analysis of TOF data in 3D space but result in loss of resolution for smaller vessels. For this reason, TOF MRA data superimposed on T1 images were also viewed in coronal, sagittal and transverse orientations. In particular, we used the sagittal orientation to improve the recognition of the small uncal branches of the AChA and the anastomosis between AChA and PCA branches in the hippocampal head, whereas the transverse orientation was analyzed to assess the anastomotic system between the AChA and PCA in the hippocampal body and tail. The coronal view is important to better investigate the hippocampal arteries from the PCA and to verify the relationships between the hippocampal arteries and the head, body and tail of the hippocampus. In the coronal plane, the three parts of the hippocampus were identified based on their morphology and by the following local radiological landmarks: the hippocampal head from the first slice of hippocampal gray matter to the uncal apex, the hippocampal body from the uncal apex to the colliculi, and the hippocampal tail from the latter to the last slice of hippocampal gray matter. As described in previous postmortem studies, the vessel diameters in the hippocampal and temporo-medial supply range widely in size, from a mean diameter of 2.6 mm for the PCA to 0.5 mm for the hippocampal arteries and 0.09 mm for the straight intrahippocampal vessels. Thus, extra and intrahippocampal vessels were roughly separated into the following four levels based on their average diameter and their possibility to be recognized in TOF data: Level 1 – PCA and AChA (detectable in all the hemispheres); Level 2 – the temporal branches from the PCA, including all the inferior temporal arteries, the CT, the lateral posterior choroidal arteries (LPChA) and the splenial artery (SplA, detectable in all the hemispheres); Level 3 – all hippocampal arteries (not always detectable, not easy to recognize, minimum diameter under TOF spatial resolution limit); and Level 4 – straight intrahippocampal arteries (never detectable, as the average diameter is approximately 1/3 of the resolution of existing TOF data) (Fig. 5). The diameters of the AChA and PCA were measured manually, followed with an automated method based on computational measures. MATLAB (R2013.b) was chosen as the programming environment. For each subject, an axial slide, which contained the anterior choroidal artery, was selected manually. According to our specifications, the axial slide had to include a tubular-shaped segment (longer than wide). A binary approach was used to separate vessels from brain background. Each region was displayed, and the artery chosen for further analysis. Using the tools at hand, we computed the minor axis length. Combining this value with the resolution of the MRI data, we obtained an approximation of the diameters of different AChAs in millimeters.

Eighty-two hemispheres were investigated to classify hippocampal and PCA vascularization patterns according to the classifications

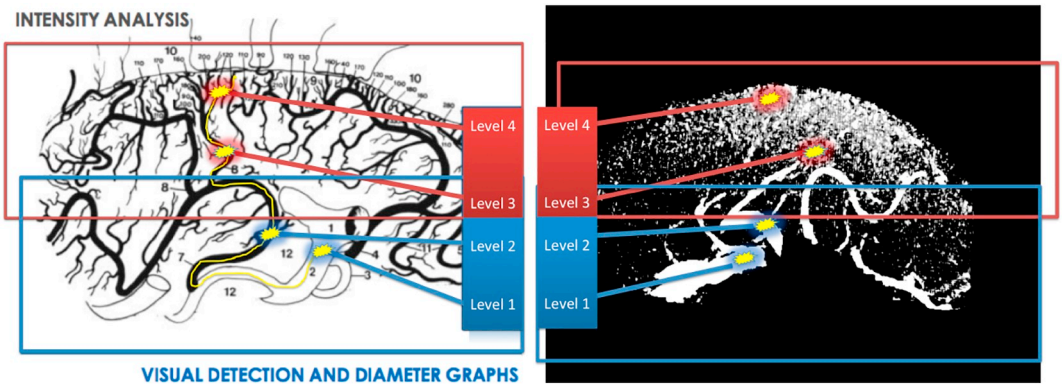

Fig. 5. Visual detection and diameter graphs *vs* intensity analysis. On the left: graphic reproduction (Marinkovic et al., 1992). On the right: 7 T MRI reconstruction. Level 1 = PCA (mean 2.6 mm), AChA (mean 0.9 mm). Level 2 = Branches from the PCA (mean 0.8 mm). Level 3 = Hippocampal arteries (mean 0.5 mm, range 0.2–0.8 mm). Level 4 = Straight intrahippocampal arteries (mean 0.09 mm). Yellow line indicates possible pathway from the PCA to intrahippocampal arteries.

Table 1
Characteristics of the hippocampal arteries. AT: anterior inferior temporal artery; PCA: posterior cerebral artery; AChA: anterior choroidal artery; CT: common trunk (common temporal artery); MT: middle inferior temporal artery; PT: posterior inferior temporal artery; LPChA: lateral posterior choroidal artery; SplA: splenial artery.

Hippocampal arteries	Main hippocampal supply	Frequency (of detection)	Parent vessels (%)	
Anterior hippocampal artery	Head and uncus	86.1% (68/79 hemispheres)	AT	42.6%
			PCA	25%
			AChA	20.6%
			AChA&AT	11.8%
Middle hippocampal artery	Body	72.1% (57/79 hemispheres)	AT	33.3%
			PCA	21.1%
			CT	24.6%
			MT	8.7%
			LPChA	12.3%
Posterior hippocampal artery	Tail	62.2% (49/79 hemispheres)	PCA	34.6%
			PT	24.5%
			SplA	24.5%
			PCA&SplA	8.2%
			PCA&PT	8.2%

established in autopsy studies. PCA and AChA branches were detected, and different vascularization patterns were estimated. All the anatomical landmarks and observations about vessels, including site of origin, direction and course in 3D space, diameters and relationships with brain structures, were used to avoid misidentifications and ensure an accurate detection of vessels.

We tried to classify the hippocampal vascularization patterns into five groups, according to Erdem's study and the origin of hippocampal vessels, and PCA patterns into three groups, following Haegalen's observations on the role of the PCA in supplying the medial temporal lobe. The classification process was performed by a neurologist with experience in angiographic analysis and was repeated multiple times with random order, to prevent biased decisions. If different choices were made for the same subject, this subject was deemed unclassifiable and was excluded from further statistics.

2.4. Statistical analysis

Statistical analyses were conducted using SPSS version 21.0 (IBM Corp, Armonk, NY). Differences between vascular patterns were assessed using one-way ANOVA (AChA diameters) and χ^2 tests (left-right distribution, relationships between the two classifications).

Concordance between the left and the right hemispheres was defined as the proportion of subjects with the same vascular pattern on both sides. The hippocampal patterns were analyzed as different subgroups (patterns from A to E) and also in a dichotomous way as pattern A + E and Pattern B + C, in order to better differentiate the AchA contribution to the hippocampal supply.

3. Results

We compared hippocampal and PCA vascular patterns with two previous autopsy studies (Erdem et al., 1993; Haegelen et al., 2012). We analyzed 82 hemispheres in total, which is more than double the number of hemispheres studied by Erdem et al. (30 hemispheres) and Haegelen et al. (40 hemispheres). We were unable to classify PCA patterns in only 3 hemispheres (4%), whereas hippocampal patterns remained unclassified in 20 hemispheres (24%). Classification failures were not due to data artifacts but resulted from a failure to track vessels of interest, *e.g.*, because of crossings with other vessels. These cases were excluded from the analysis. For all other hemispheres, we found good agreement between hippocampal and PCA vascular patterns in our study and the two aforementioned autopsy studies.

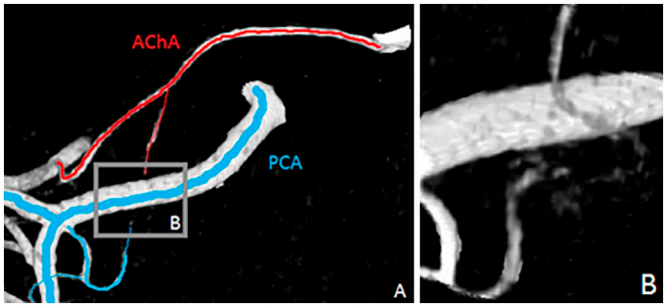

Fig. 6. Extrahippocampal anastomoses. A) AChA and PCA branches at the level of the uncal sulcus B) anastomoses between AChA and PCA branches.

3.1. Medial temporal and hippocampal arteries

The anterior temporal (AT) and the posterior temporal artery (PT) were found in all the hemispheres except when a common trunk (CT) was present (n = 60, 76%). A CT, characterized by a common origin of all the cortical branches of the PCA, was seen in the remaining hemispheres (n = 19, 24%). The middle temporal artery was found in only 15 hemispheres (19%). The anterior hippocampal arteries (AH) were the most frequently detected (86.1%), followed by the middle (MH, 72.1%), and posterior hippocampal arteries (PH, 62.2%) (Table 1). The AH supplied the hippocampal head and the uncus and mainly arose from the AT (42.6%) and PCA (25%). The AT (33.3%) and PCA (21.1%), together with the CT (24.6%), were the main sites of origin for the MH. PH arose from the PCA (34.6%), PT (24.5%) and SplA (24.5%) and had a higher frequency of multiple vessels than the AH and MH.

3.2. Extrahippocampal anastomoses

While considering the resolution limit of our angiograms, we were able to identify the two main sites of anastomoses between the AChA and PCA system in the anterior hippocampus and the transition between the mid- and posterior hippocampus. In the anterior hippocampus, anastomoses were located in the uncal sulcus and consisted of the AH, provided by the PCA (or its branches), and the AChA, usually by its uncal branches (Fig. 6). In the transition between the mid- and posterior hippocampus, at the level of the lateral geniculate body, we observed anastomoses between AChA and LPChA branches. The identification of anastomoses was not reliable enough to quantify their frequency.

Table 2
Classification of the hippocampal patterns according to the origin of the hippocampal arteries. AChA: anterior choroidal artery; PCA: posterior cerebral artery.

Group	Origin of hippocampal supply	Contribution of the AChA	Neurosurgical study	TOF MRA data
			30 hemispheres (Erdem et al., 1993)	62 hemispheres
A	Mixed origin from the AChA and PCA branches	Yes	17 (57%)	31 (50%)
B	Mainly from all the inferior temporal branches of the PCA	No	8 (27%)	21 (34%)
C	Mainly from the anterior inferior temporal artery of the PCA	No	3 (10%)	7 (11%)
D	Directly from the PCA trunk	No	1 (3%)	0 (0%)
E	Mainly from the AchA branches	Yes	1 (3%)	3 (5%)

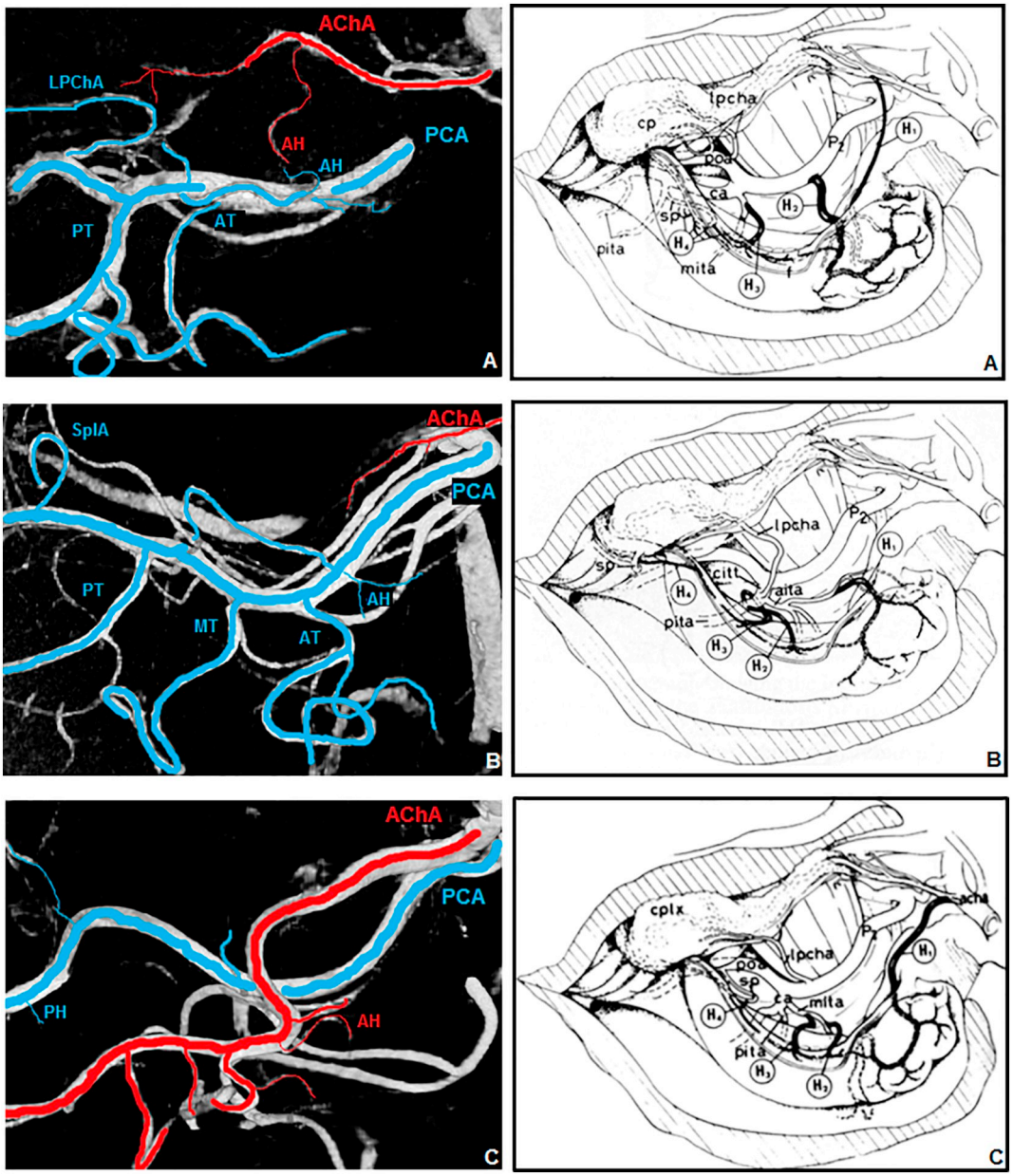

Fig. 7. Hippocampal patterns. On the left: 7 T TOF MRA reconstruction; on the right: graphic reproduction (Erdem et al., 1993). A) Pattern A (mixed supply PCA plus AChA); B) Pattern B (mainly from PCA); C) Pattern E (mainly from AChA). PCA and its branches (blue); AChA and its branches (red). PCA: posterior cerebral artery; AChA: anterior choroidal artery; AT: anterior inferior temporal artery; MT: middle inferior temporal artery; PT: posterior inferior temporal artery; LPChA: lateral posterior choroidal artery; SplA: splenial artery, AH anterior hippocampal artery; PH posterior hippocampal artery.

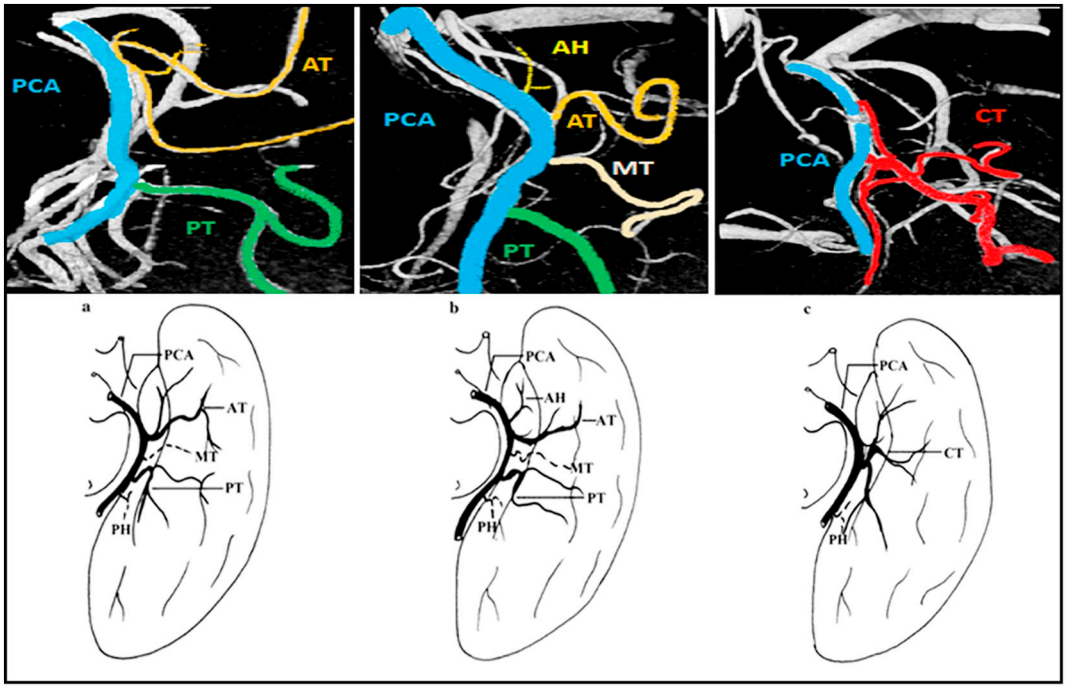

Fig. 8. PCA Patterns. Above: 7 T TOF MRA visualization; below: graphic reproduction (Haegelen et al., 2012). Pattern 1 (AT + PT); Pattern 2 (AH + AT + PT); Pattern 3 (CT). AH: anterior hippocampal artery; AT: anterior inferior temporal artery; MT: middle inferior temporal artery; PT: posterior inferior temporal artery; CT: common trunk (common temporal artery); PCA posterior cerebral artery.

Table 3
Classification of the inferior temporal branches of the PCA. AH: anterior hippocampal artery; AT: anterior inferior temporal artery; PT: posterior inferior temporal artery; CT: common trunk (common temporal artery).

Pattern	Common Point	Neurosurgical study	TOF MRA data
		40 hemispheres (Haegelen et al., 2012)	79 hemispheres
1	AT + PT	23 (57.5%)	43 (54%)
2	AH + AT + PT	9 (22.5%)	17 (22%)
3	CT	8 (20%)	19 (24%)

3.3. Hippocampal patterns

In 62 of 82 hemispheres, we classified the different hippocampal vascularization patterns based on the origin of the hippocampal artery supply. Compatible with Erdem et al. (1993), Pattern A (PCA + AChA) was found most frequently ($n = 31$, 50%), followed by Pattern B (mainly PCA branches, including all the inferior temporal branches, $n = 21$, 34%), Pattern C (PCA branches, mainly from the anterior inferior temporal artery, $n = 7$, 11%) and Pattern E (mainly AChA branches, n = 3, 5%) (Table 2). We did not find pattern D (hippocampal arteries that arise directly from the PCA trunk), which was observed only once in the sample of Erdem et al. (1993). Thus, overall, AChA contribution to hippocampal vascularization was found in 34 of 62 hemispheres (patterns A + E), while in the remaining hemispheres, we could identify only an origin of hippocampal arteries from PCA or PCA branches (Pattern B + C) (Fig. 7).

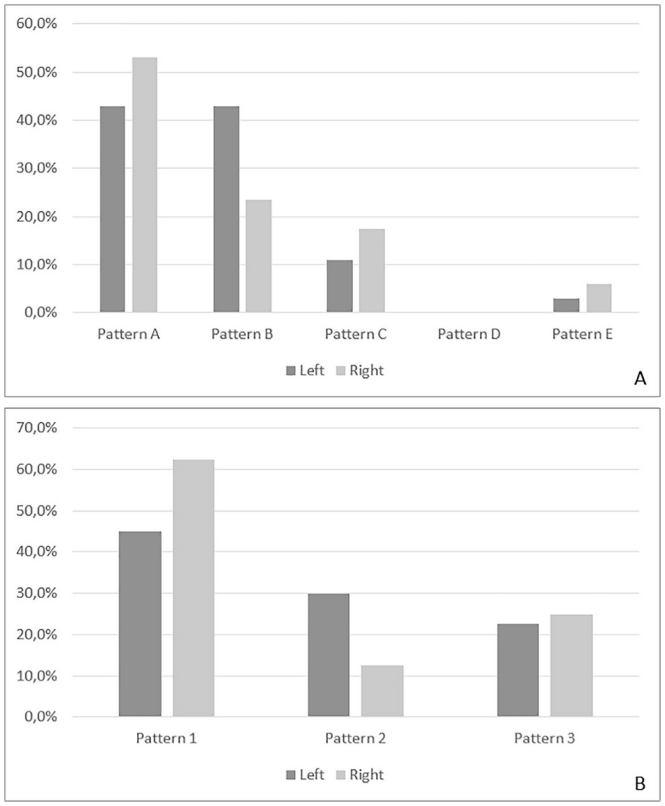

Fig. 9. Vascular patterns of the left and right hemisphere. A) Hippocampal patterns; B) PCA patterns.

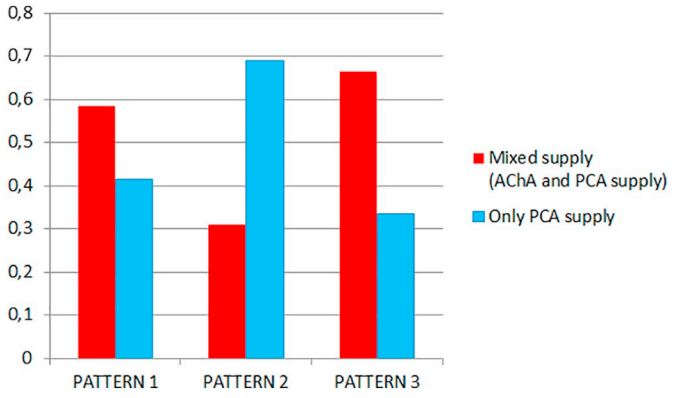

Fig. 10. Relationships between hippocampal and PCA Patterns. Mixed supply (AChA and PCA supply, hippocampal patterns A and E) (red); PCA supply (hippocampal patterns B and C) (light blue). PCA Patterns 1, 2 and 3 according to Haegelen et al., 2012.

3.4. PCA patterns

In 79 of 82 hemispheres, we classified the inferior temporal cortical branches of the PCA according to the autopsy study provided by Haegelen et al. (2012). Pattern 1 (AT + PT, without AH) was the most frequent (n = 43, 54%), followed by Pattern 3 (CT, n = 19, 24%) and Pattern 2 (AH + AT + PT, n = 17, 22%) (Fig. 8, Table 3).

3.5. Lateralization of vascularization patterns

The concordance between the left and right hemispheres was 79% for hippocampal patterns (considered Pattern A + E *versus* Pattern B + C; 26 of 33 subjects) but only 44% for PCA patterns (17 of 39 subjects). Among hippocampal patterns, we did not find any statistically significant difference in the distribution, with only a slight predominance of Pattern A in the right hemisphere (p 0.092) and Pattern B in the left hemisphere (p 0.066). Within PCA patterns, Pattern 2 was more frequent in the left hemisphere ($p < .05$) (Fig. 9).

3.6. AChA diameters and relationships between hippocampal and PCA patterns

We observed some anatomical relationships between the two classifications (PCA patterns from Haegelen et al., 2012 and hippocampal patterns from Erdem et al., 1993) (Fig. 10). PCA patterns 1 and 3 were more frequently associated with a mixed supply of the hippocampus (AChA + PCA, patterns A and E), whereas with PCA Pattern 2, the hippocampal supply more frequently depended only on the PCA (patterns B and C) ($p < .05$). When the AH arose directly from the PCA, as in Pattern 2, we observed a lower contribution of the AChA to hippocampal vascularization. Additionally, there were fewer anastomoses between the AChA and PCA systems in both the uncal sulcus and between the LPchA (branches from PCA) and AChA. In this scenario, the PCA supplies not only the medial and posterior parts of the hippocampus but also the hippocampal head and the uncus, which are usually well vascularized by the AChA. The automated detection of the diameter of the AChA seemed to confirm these observations. Although not statistically significant (mean 1.23 mm ± 0.28, p 0.132), we found that the mean diameter of the AChA in Pattern 3 (1.32 mm) is larger than those in patterns 1 (1.21 mm) and 2 (1.18 mm). Moreover, we observed that the diameter of the AChA was significantly correlated with a mixed supply of the hippocampus (Pattern A and E) ($p < .01$).

4. Discussion

To the best of our knowledge, this study is the first to describe the different vascularization patterns of the human hippocampus *in vivo*. While considering the limitations of a 7 T TOF study compared with autopsy studies, the strong concordance with neurosurgical data seems to confirm the accuracy of our classification. However, the resolution limit of 0.3 mm of the current protocol was under the minimum diameter of the hippocampal arteries (minimum 0.2 mm, range 0.2–0.8 mm), and a complete count of the hippocampal arteries was not possible and thus beyond the scope of this study. The intrahippocampal arteries (mean diameter 0.09 mm) are well below the resolution limit of current 7 T TOF images, and the intrahippocampal vascular network can be detected only indirectly by intensity analysis. Another possible limitation of the study is inherent to our visualization method. To assure good accuracy and methodological rigor, we repeated the image analysis multiple times, in random order and blind to previous results, and we excluded conflicting classifications from the final results. However, given the high complexity of the classifications and the substantial anatomical knowledge required, the study may not be easily reproducible. With the current angiographic imaging protocol and our processing and visual inspection procedure, the PH, MH, and AH were detected in 62.2%, 72.1% and 86.1% of the hemispheres (Table 1). The differences in detection were caused by the greater vascular complexity in the body and tail of the hippocampus, where multiple arteries were often observed and arose from various different parental vessels. However, our description of the hippocampal arteries, in terms of type and frequency of the parental vessels, is consistent with the previous observations of Marinkovic et al. (1992). As suggested by Erdem et al. (1993), given the high variability in the number of hippocampal arteries, systematization based on only the number of hippocampal arteries seems impracticable, and according to his work, we classified hippocampal vascularization on the basis of the origin of hippocampal arteries and the contribution of the AChA to the hippocampal supply (Table 2). As seen in our classification, the hippocampus can be supplied by either the PCA and its branches or from a combination of the PCA and AChA branches. If the PCA always supplies the hippocampus, the contribution of the AChA is highly variable and displays close relationships with different PCA patterns involved in the medial temporal supply. For instance, we found that when the temporal cortical branches of the PCA arise from a CT, most of the supply of the hippocampal head is usually provided by the AChA. On the other hand, if the AH arises directly from the PCA, the AChA is frequently small and engenders fewer branches to the hippocampus. These results seem to confirm how the different hippocampal patterns strictly affect hippocampal supply, particularly in its head. The different contributions of the AChA to hippocampal vascularization and the resulting mixed supply of the hippocampus (Patterns A and E) may be an important determinant of hippocampal perfusion. This result led us to the hypothesis that the diameter of the AChA could correlate with the existing hippocampal and medial temporal pattern, by providing an easier neuroimaging marker for the vascularization patterns detection. When the AChA is larger and significantly contributes to the hippocampal blood supply, we observed that the anastomoses between the AChA and PCA branches were more evident, especially in the uncal sulcus.

The interindividual variability in the hippocampal supply and the efficiency of the extrahippocampal anastomoses may have a role in the ability of the hippocampus to cope with hypoperfusion and anoxia. Considering the suspected intrinsic fragility of the intrahippocampal vascular network (Duvernoy, 2005; Duvernoy et al., 1981), speculating that different vascular patterns may represent either a risk or protective factor in some particular conditions associated with hippocampal

degeneration may not be too bold. For example, one hallmark of Alzheimer's disease (AD) is hippocampal atrophy (Caroli and Frisoni, 2010; Jack Jr et al., 1997), concordant with the molecular pathology of Alzheimer's disease which is known to include the entorhinal cortex and the hippocampus early in the disease (Braak and Braak, 1995; Arnold et al., 1991). Vascular risk factors have an important impact on the sporadic form of AD (Breteler, 2000; Fratiglioni et al., 2004; Qiu et al., 2010) and in determining alterations in the deposition and clearance of amyloid pathology (De la Torre, 2004; Gupta and Iadecola, 2015; Toledo et al., 2013) by means of metabolic (Sato and Morishita, 2015) and hemodynamic effects (Hughes et al., 2014; Okamoto et al., 2012). These latter effects play causal roles in hypoperfusion, reduced vasomotor reactivity and cerebral autoregulation (den Abeelen et al., 2014). In this scenario, vascular hippocampal patterns may be a new variable to consider to better understand the individual phenotypic relationships between vascular and degenerative pathology in AD patients. Additionally, the link between physical exercise and cognition could be influenced by individual differences in vascular anatomy. Recent studies have shown that physical exercise can induce neuronal and vascular plasticity in the hippocampus (Erickson et al., 2011; Voss et al., 2010; Whiteman et al., 2016). In a 7 T study performed by our group (Maas et al., 2015), we observed that fitness improvement correlates with changes in hippocampal perfusion and head volume and that aerobic exercise can induce vascular plasticity in older adults. However, we and others (for a review see Düzel et al., 2016) have also observed that there is considerable interindividual variability in the response to the physical exercise which is still poorly understood. Indeed, some older individuals even show decreased hippocampal perfusion after aerobic exercise (Iadecola, 2015). Hence, individual differences in hippocampal vascularization may explain some of the individual variability in response to exercise.

In this study, through the use of 7 T TOF angiography, we have demonstrated for the first time the detection of the different vascular patterns involved in the hippocampal blood supply. In the early twentieth century, the laboratories of Spielmeyer and Vogts provided the first evidence of a connection between vascular anatomy and hippocampal pathology. Currently, after almost one hundred years, 7 T MRI technology may allow us to validate those findings and to correlate vascular supply profiles with clinical and functional data *in vivo*.

5. Conclusions

The ability to compare *in vivo* individual differences in hippocampal vascularization with perfusion and clinical data may represent an important first step to better clarify the relationship between vascular and degenerative pathology in the hippocampus. Moreover, our results may provide further information about hippocampal angiographic patterns and their contributions to other research areas, such as physical training effects and cognition.

Acknowledgments

This research was supported by the BMBF (“EnergI” Consortium). The authors declare no conflicts of interest.

References

Arnold, S.E., Hyman, B.T., Flory, J., Damasio, A.R., Van Hoesen, G.W., 1991. The topographical and neuroanatomical distribution of neurofibrillary tangles and neuritic plaques in the cerebral cortex of patients with Alzheimer's disease. Cereb. Cortex 1, 103–116.

Avants, B.B., Tustison, N.J., Song, G., Cook, P.A., Klein, A., Gee, J.C., 2011. A reproducible evaluation of ANTs similarity metric performance in brain imaging registration. NeuroImage 54, 2033–2044.

Blümcke, I., Beck, H., Lie, A.A., Wiestler, O.D., 1999. Molecular neuropathology of human mesial temporal lobe epilepsy. Epilepsy Res. 36, 205–223.

Braak, H., Braak, E., 1995. Staging of Alzheimer's disease-related neurofibrillary changes. Neurobiol. Aging 16, 271–278 Review.

Breteler, M.M., 2000. Vascular risk factors for Alzheimer's disease: an epidemiologic perspective. Neurobiol. Aging 21, 153–160.

Caroli, A., Frisoni, G.B., 2010. Alzheimer's disease neuroimaging initiative the dynamics of Alzheimer's disease biomarkers in the Alzheimer's disease neuroimaging initiative cohort. Neurobiol. Aging 31, 1263–1274.

De la Torre, J.C., 2004. Is Alzheimer's disease a neurodegenerative or a vascular disorder? Data, dogma, and dialectics. Lancet Neurol. 3, 184–190.

Duvernoy, H.M., 2005. The Human Hippocampus: Functional Anatomy, Vascularization and Serial Sections with MRI. Springer Verlag, Berlin Heidelberg.

Duvernoy, H., Delon, S., Vannson, J.L., 1981. Cortical blood vessels of the human brain. Brain Res. Bull. 7, 519–579.

Düzel, E., van Praag, H., Sendtner, M., 2016. Can physical exercise in old age improve memory and hippocampal function? Brain 139, 662–673.

Erdem, A., Gazi Yasargil, M., Roth, P., 1993. Microsurgical anatomy of the hippocampal arteries. J. Neurosurg. 79, 256–265.

Erickson, K.I., Voss, M.W., Prakash, R.S., Basak, C., Szabo, A., Chaddock, L., Kim, J.S., Heo, S., Alves, H., White, S.M., 2011. Exercise training increases size of hippocampus and improves memory. Proc. Natl. Acad. Sci. U. S. A. 108, 3017–3022.

Fernandez-Miranda, J.C., de Oliveira, E., Rubino, P.A., Wen, H.T., Rhoton, A.L., 2010. Microvascular anatomy of the medial temporal region: part 1: its application to arteriovenous malformation surgery. Neurosurgery 67, 237–276.

Fratiglioni, L., Paillard-Borg, S., Winblad, B., 2004. An active and socially integrity lifestyle in late light might protect against dementia. Lancet Neurol. (6), 343–353.

Gastaut, H., Lammers, J.H., 1961. Anatomie du rhinencephale. Masson Paris.

Gupta, A., Iadecola, C., 2015. Impaired Ab clearance: a potential link between atherosclerosis and Alzheimer's disease. Front. Aging Neurosci. 7, 115.

Haegelen, C., Berton, E., Darnault, P., Morandi, X., 2012. A revised classification of the temporal branches of the posterior cerebral artery. Surg. Radiol. Anat. 34, 385–391.

Heverhagen, J.T., Bourekas, E., Sammet, S., Knopp, M.V., Shmalbrock, P., 2008. Time-of-flight magnetic resonance angiography at 7 Tesla. Investig. Radiol. 43, 568–573.

Hughes, T.M., Kuller, L.H., Barinas-Mitchell, E.J., McDade, E.M., Klunk, W.E., Cohen, A.D., Mathis, C.A., Dekosky, S.T., Price, J.C., Lopez, O.L., 2014. Arterial stiffness and b-amyloid progression in non demented elderly adults. JAMA Neurol. 71, 562–568.

Huther, G., Dorfl, J., Van der Loos, H., Jeanmonod, D., 1998. Microanatomic and vascular aspects of the temporomesial region. Neurosurgery 43, 1118–1136.

Iadecola, C., 2015. Dangerous leaks: blood-brain barrier woes in the aging hippocampus. Neuron 85, 231–233.

Jack Jr., C.R., Petersen, R.C., Xu, Y.C., O'Brien, P.C., Smith, G.E., Ivnik, R.J., Tangalos, E.G., Kokmen, E., 1997. Medial temporal atrophy on MRI in normal aging and very mild Alzheimer's disease. Neurology 49, 786–794.

Klosovskii, B.N., 1963. Fundamental principles of the development, structure and function of the vaso-capillary network of the brain. In: Klosovskii, B.N. (Ed.), The Development of the Brain and Its Disturbance by Harmful Factors. Pergamon, Oxford, pp. 44–54.

Maas, A., Duzel, S., Goerke, M., Becke, A., Sobieray, U., Neumann, K., Lovden, M., Lindenberger, U., Backman, L., Braun-Dullaeus, R., Ahrens, D., Heinze, H.J., Muller, N.G., Duzel, E., 2015. Vascular hippocampal plasticity after exercise in older adults. Mol. Psychiatry 20, 583–593.

Marinkovic, S., Milisavljevic, M., Puskas, L., 1992. Microvascular anatomy of the hippocampal formation. Surg. Neurol. 37, 339–349.

Marinkovic, S., Gibo, H., Brigante, L., Nikodijevic, I., Petrovic, P., 1999. The surgical anatomy of the perforating branches of the anterior choroidal artery. Surg. Neurol. 52, 30–36.

Morandi, X., Brassier, G., Darnault, P., Mercier, P., Scarabin, J.M., Duval, J.M., 1996. Microsurgical anatomy of the anterior choroidal artery. Surg. Radiol. Anat. 18, 275–280.

Muller, J., Shaw, L., 1965. Arterial vascularization of the human hippocampus. 1. Extracerebral relationships. Arch. Neurol. 13, 45–47.

den Abeelen, A.S., Lagro, J., van Beek, A.H., Classsen, J.A., 2014. Impaired cerebral autoregulation and vasomotor reactivity in sporadic Alzheimer's disease. Curr. Alzheimer Res. 11, 11–17.

Okamoto, Y., Yamamoto, T., Kalaria, R.N., Senzaki, H., Maki, T., Hase, Y., Kitamura, A., Washida, K., Yamada, M., Ito, H., Tomimoto, H., Takahashi, R., Ihara, M., 2012. Cerebral hypoperfusion accelerates cerebral amyloid angiopathy and promotes cortical microinfarcts. Acta Neuropathol. 123, 381–394.

Patenaude, B., Smith, S.M., Kennedy, D.N., Jenkinson, M.A., 2011. Bayesian model of shape and appearance for subcortical brain segmentation. NeuroImage 56, 907–922.

Qiu, C., Xu, W., Winblad, B., Fratiglioni, L., 2010. Vascular risk profiles for dementia and Alzheimer's disease in very old people: a population based longitudinal study. J. Alzheimers Dis. 20, 293–300.

Ravens, J.R., 1974. Anastomoses in the vascular bed of the human cerebrum. In: Cervos Navarro, J. (Ed.), Pathology of Cerebral Microcirculation. De Gruyter, Berlin, pp. 26–38.

Rothman, S.M., 1984. Synaptic activity mediates death of hypoxic neurons. Science 220, 536–537.

Sato, N., Morishita, R., 2015. The roles of lipid and glucose metabolism in modulation of b-amyloid, tau, and neurodegeneration in the pathogenesis of Alzheimer disease. Front. Aging Neurosci. 7, 199.

Scharrer, E., 1940. Vascularization and vulnerability of the cornu ammonis in the opossum. Arch. Neurol. Psychiatr. 44, 483–506.

Selle, D., Preim, B., Schenk, A., Peitgen, H.O., 2002. Analysis of vasculature for liver surgical planning. IEEE Trans. Med. Imaging 21, 1344–1357.

Spielmeyer, W., 1925. Zur Pathogenese örtlich elektiver Gehirnveränderungen Zeitschrift für die gesamte. Neurol. Psychiatr. 99, 756–776.

Spielmeyer, W., 1927. Die pathogenese des epileptischen Krampfes. Zeitschrift für die gesamte. Neurologie und Psychiatrie 109, 501–520.

Toledo, J.B., Arnold, S.E., Raible, K., Brettschneider, J., Xie, S.X., Grossman, M., Monsell, S.E., Kukull, W.A., Trojanoswki, J.Q., 2013. Contribution of cerebrovascular disease in autopsy confirmed neurodegenerative disease cases in the National Alzheimer's Coordinating Centre. Brain 136, 2697–2706.

Uchimura, J., 1928. Über die Gefäßversorgung des Ammonshornes Zeitschrift für die gesamte. Neurol. Psychiatr. 112, 1–19.

Vogt, C., Vogt, O., 1937. Sitz und Wesen der Krankheiten im Lichte der topistischen Hirnforschung und des Variierens der Tiere. J. Psychol. Neurol. 47, 237–457.

Voss, M.W., Prakash, R.S., Erickson, K.I., Basak, C., Chaddock, L., Kim, J.S., Alves, H., Heo, S., Szabo, A., White, S.M., Wojcicki, T.R., Mailey, E.L., Gothe, N., Olson, E.A., McAuley, E., Kramer, A.F., 2010. Plasticity of brain networks in a randomized intervention trial of exercise training in older adults. Front. Aging Neurosci. 2, 1–17.

Wen, H.T., Rhoton, A.L., de Oliveira, E., Cardoso, A.C., Tedeschi, H., Baccanelli, M., Marino, R., 1999. Microsurgical anatomy of the temporal lobe: part 1: mesial temporal lobe anatomy and its vascular relationships as applied to amygdalohippocampectomy. Neurosurgery 45, 549–591.

Whiteman, A.S., Young, D.E., Budson, A.E., Stern, C.E., Schon, K., 2016. Entorhinal volume, aerobic fitness, and recognition memory in healthy young adults: a voxelbased morphometry study. NeuroImage 126, 229–238.

Zang, Z., Deng, X., Weng, D., An, J., Zuo, Z., Wang, B., Wei, N., Zhao, J., Xue, R., 2015. Segmented TOF at 7T MRI: Technique and clinical applications. NeuroImage 33, 1043–1050.

Zeal, A.A., Rhoton, A.L., 1978. Microsurgical anatomy of the posterior cerebral artery. J. Neurosurg. 48, 534–555.